IEEE Journal of Photovoltaics, doi: 10.1109/JPHOTOV.2019.2933185

Influence of Room Temperature Sputtered Al-doped Zinc Oxide on Passivation Quality in Silicon Heterojunction Solar Cells

Huimin Li, Weiyuan Duan*, Andreas Lambertz, Jürgen Hüpkes, Kaining Ding, Uwe Rau, and Oleksandr Astakhov

***Abstract*— Al-doped zinc oxide (AZO) is a potential candidate to substitute tin-doped indium oxide (ITO) in silicon heterojunction (SHJ) solar cells due to its low cost and low ecological impact. The AZO, sputtered at room temperature (RT), is of particular interest because of low thermal budget and potential for high throughput production with the well-established industrial methods. In SHJ solar cells high effective carrier lifetime prerequisite for the high open-circuit voltage is achieved with surface passivation by intrinsic amorphous silicon layers followed by doped silicon layers. The passivation quality may be affected by the subsequent sputtering of an AZO layer especially at RT. In this work, we investigated the influence of the AZO sputtering and post-deposition annealing on the effective carrier lifetime in symmetrical silicon layer stacks with n- or p-type doped silicon layers and solar cell precursors. It has been found that the effective carrier lifetime significantly decreased after AZO sputtering at RT. The detrimental effect of AZO sputtering is substrate temperature dependent and is smaller or even absent at elevated temperatures. However post-deposition annealing, equivalent to the Ag paste curing, mostly recovered the effective carrier lifetime in the symmetrical stacks as well as in the cell precursors. Finally an aperture area efficiency of 21.2 % has been achieved for the 19 mm × 19 mm SHJ solar cell prepared with room temperature sputtered AZO.**

***Index Terms*—Charge carrier lifetime, Crystalline Silicon PV, Heterojunctions, PV Si Defect Passivation and Advanced Optics, Sputtering**

I. Introduction

SILICON heterojunction (SHJ) solar cells with amorphous silicon passivation layers deposited on monocrystalline silicon wafers show very high efficiencies in the traditional double-side contacted design [1]-[3] and hold the absolute efficiency record among single junction silicon solar cells in back-side contacted configuration [4]. Design of a SHJ solar cell includes transparent conductive oxide (TCO) layers deposited on top of doped silicon layers on the front and rear sides of the device. These TCO layers facilitate lateral conductance for efficient current collection and simultaneously serve as antireflection coatings. Tin-doped indium oxide (ITO) is commonly used as TCO material in SHJ solar cells thanks to its excellent optical and electrical properties [5], [6]. However, ITO may be challenging for the mass production of SHJ solar cells due to indium related economic and environmental issues [7]-[10]. Al-doped zinc oxide (AZO), which is environmentally friendly, abundant and less costly material, is an attractive alternative to ITO in SHJ solar cells [11]-[13]. Magnetron sputtered AZO is a widely used TCO for various solar cell technologies. Many studies [13]-[20] have presented the potential of implementing AZO deposited at elevated temperature (50-300 ^{o}C) in SHJ solar cells. Considering mass production requirements, we explore the potential of implementing AZO prepared at room temperature (RT) with common magnetron sputtering technique in SHJ solar cells. Huang *et al*. [21] have reported the detailed analysis of ITO deposition damage mechanism in SHJ solar cells. However, there are few reports on the influence of AZO sputtering on solar cells stacks. In this work, we address the influence of AZO sputtering on the effective carrier lifetime (τ_{eff}) in the symmetrical structures as well as in SHJ solar cell precursors. Finally the potential of RT sputtered AZO as TCO in SHJ solar cells is explored.

In a conventional SHJ solar cell doped amorphous (a-Si:H) layers are typically used to form the p-n junction and back surface field. Doped a-Si:H layers form a proper ohmic contact with commonly used ITO, however, a-Si:H may be less suitable material for contact with AZO [13]. Nanocrystalline silicon (nc-Si:H) doped layers are expected to be more suitable in contact with AZO, and have a potential to reduce parasitic absorption. In this work SHJ solar cells with n-type nc-Si:H (nc-Si:H<n>) layer in rear emitter configuration were studied in continuation of the experiments reported earlier [22]. It has been found that the preparation of RT sputtered AZO may have a detrimental effect on the effective carrier lifetime which causes losses in V_{oc} and FF of the SHJ solar cells. Here we present a detailed study on the influence of the AZO sputtered at different pressures and temperatures on the effective carrier

This work was supported by the HEMF (Helmholtz Energy Materials Foundry) infrastructure funded by the (HGF) Helmholtz association, China Scholarship Council (CSC) and the Bundesministerium für Wirtschaft und Energie in the network project "PATOS" [FKZ 0324074E].

The Authors are with IEK-5 Photovoltaik, Forschungszentrum Jülich GmbH, Jülich, Nordrhein-Westfalen, 52425, Germany (e-mail: h.li@fz-juelich.de; w.duan@fz-juelich.de; a.lambertz@fz-juelich.de; j.huepkes@fz-juelich.de; k.ding@fz-juelich.de; u.rau@fz-juelich.de; o.astakhov@fz-juelich.de).

lifetime in SHJ solar cells. We demonstrate that the effective carrier lifetime degradation, related to AZO sputtering, can be reduced or avoided by a subsequent annealing. This annealing is similar to the typical silver paste curing which is a necessary part of a SHJ cell production. Alternatively AZO sputtering at elevated substrate temperature facilitates in-situ annealing reducing or eliminating the sputtering damage.

II. Experimental Details

Fig. 1 shows the schematic illustration of the SHJ solar cells fabricated for our study. The cells were prepared in rear junction configuration, i.e., an n-type silicon layer was used as window layer at the front of the device, and the p-n junction was formed at the rear side. The cells were prepared on n-type double side textured Czochralski (CZ) silicon wafers with the thickness of 170 µm and resistivity of 0.5-3.5 Ω·cm. The wafers were chemically cleaned with RCA Standard Clean 1 (NH_4OH: H_2O_2: deionized water), RCA Standard Clean 2 (HCl: H_2O_2: deionized water) and subsequently dipped into 1 % HF solution for 5 min to remove the surface oxide. After rinsing and drying, the wafers were swiftly transferred to the plasma enhanced chemical vapor deposition (PECVD) system for silicon layer deposition. Silane, hydrogen, phosphine and trimethylborane were used as the precursor gases for the silicon layers deposited at 200 °C.

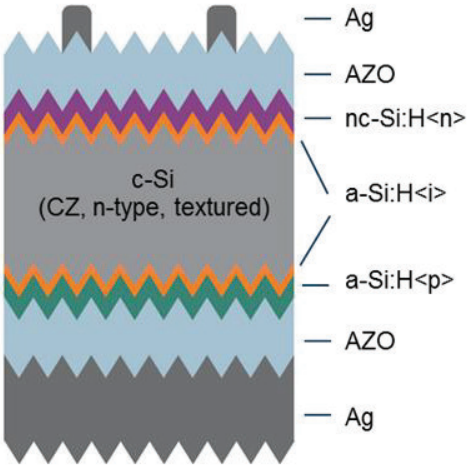

Fig. 1. Schematic illustration of rear emitter SHJ solar cells with nc-Si:H<n> layer and RT sputtered AZO

AZO films for the pressure series were prepared at RT with gas pressure of 0.1 Pa, 0.3 Pa, and 0.5 Pa. The films for the substrate temperature series were sputtered at RT, 150 °C, and 200 °C with the pressure of 0.1 Pa. All AZO depositions were performed in a vertical in-line sputtering system by radio frequency sputtering of $ZnO:Al_2O_3$ (99:1 wt. %) planar ceramic target, with 100 sccm Argon gas flow rate, and 2.0 W/cm^2 power density related to the target area of 75 cm × 10 cm. The depositions were performed in dynamic mode with a carrier moving back and forward in front of the target at the speed of 5.1 mm/s. In order to study the AZO properties, the films were sputtered on Corning EAGLE XG glass substrate. The AZO film thickness of approximately 80 nm corresponds to the thickness applied in SHJ solar cells. Silver electrodes were screen-printed to finalize the cells with the aperture area of 19 mm × 19 mm. The cell aperture is defined by a square busbar frame. The contact grids in the aperture are a set of fingers with the width of 50-60 µm and the pitch of 1.85 mm. After the screen printing the cells were annealed for 40 min at 190 °C in air for silver paste curing. Finalized cells are characterized under standard test condition (25°C, AM 1.5, 100 mW/cm^2) using "LOANA" characterization setup from pv-tools equipped with a SINUS 220 Wavelabs light source. External quantum efficiency (EQE) and reflection spectra are measured by the same setup with the illuminating spot size of 12 mm × 12 mm on the cell aperture area.

Carrier mobility μ, carrier concentration n and resistivity ρ of AZO films deposited on glass substrates have been extracted from Hall measurements. Transmittance T and reflectance R of AZO films was measured with a dual beam photo spectrometer Lambda 950 in the wavelength range of 300-1300 nm. Absorptance A was calculated as $A = 1 - T - R$.

Effective carrier lifetime in the wafers with silicon layer stacks was measured by Quasi Steady-State Photo Conductance (QSSPC) technique with Sinton WCT-120 instrument in transient mode. The values for the effective carrier lifetime τ_{eff} presented in the manuscript are taken at the excess carrier density of 10^{15} cm^{-3}. Implied open circuit voltage (iV_{oc}) and implied fill factor (iFF) were evaluated from the effective carrier lifetime measurements. In addition to solar cells sketched in Fig. 1, symmetrical structures with a-Si:H<i>/nc-Si:H<n> (i/n stack) or a-Si:H<i>/a-Si:H<p> (i/p stack) on both sides of the wafer have been prepared to study individual impact of AZO sputtering and annealing on the passivation quality of front and rear layer stacks of the cell.

III. Results And Discussion

A. AZO Films

Optical transmittance and reflectance spectra of AZO films used in the study have been reported earlier [22]. Without considering the absorptance and reflectance of the glass substrate, the average absorptance in the 300-1200 nm wavelength range is 5 %, and the value can be as low as 0.5 % in the wavelength range of 400-1200 nm. The subsequent annealing at 180 °C for 30 min in air has only marginal effect on the optical properties.

Resistivity of the characterized as-deposited AZO film was 1.8×10^{-3} Ω·cm with charge carrier mobility of 16.7 cm^2/Vs, and carrier concentration of 2.2×10^{20} cm^{-3}. The resistivity is reduced after annealing to 1.2×10^{-3} Ω·cm with the increase in carrier mobility to 18.8 cm^2/Vs, and in carrier concentration to 2.9×10^{20} cm^{-3}. The improvement in electrical properties after annealing is attributed in literature to the improvement in the microstructure of AZO films [23]-[25]. The AZO sheet resistance of approximate 150 Ω/sq is on par with recent literature reports [19]. Even though the AZO sheet resistance is higher than it for the best ITO, the AZO application in SHJ solar cells is still not the major limitation for the achieving high efficiency SHJ solar cells [26]. In the view of both optical and

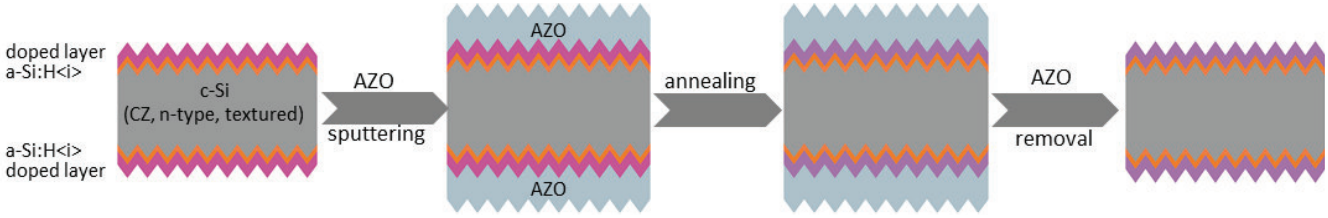

Fig. 2. Treatment procedures on i/n and i/p symmetrical stacks with doped silicon layers in the sequence: silicon layer stack deposition - AZO sputtering - annealing - AZO removal

electrical properties, AZO film sputtered at room temperature is suitable for the application as TCO in SHJ solar cells.

B. The Influence of AZO on Silicon Layer Passivation

In order to investigate the effect of AZO sputtering on the effective carrier lifetime, QSSPC measurements have been performed on the symmetrical silicon stacks after silicon layer deposition, AZO sputtering, and annealing with the process sequence presented in Fig. 2. The same procedure has been applied to the SHJ solar cell precursors as well (section *C*). Every new layer prepared on silicon layer stack may change the effective carrier lifetime either due to the impact of the preparation process on the existing layers, or the properties of the new layer itself, e.g. via field effect. In this case AZO sputtering process may damage the underlying layers and at the same time the presence of AZO film may change occupation of the electronic states in the interface region. Both effects can result in the variation of the effective carrier lifetime. In order to separate the impact of AZO sputtering from the effect of AZO presence, the AZO films were removed by 0.5 % HCl solution after annealing (shown as the last step in Fig. 2).

The wet chemical etching was chosen as a robust and simple method to remove AZO, however, it is known that exposure of thin film silicon layers to air or aqueous solutions may influence conductivity [27], [28] or charge state of defects in thin film silicon layers [29] which in turn may influence the effective carrier lifetime. In order to study possible influence of HCl solution etching on the effective carrier lifetime, QSSPC measurements were conducted before and after i/n and i/p stacks exposed to the 0.5% HCl solution. In Fig. 3 the results of QSSPC measurements and evaluated implied cell parameters are presented for both i/n and i/p symmetrical stacks before and after the HCl exposure. It can be seen that for both i/n and i/p stacks, exposure to 0.5% HCl solution has no influence on the measured effective carrier lifetime curves or the values of τ_{eff}, iV_{oc}, and iFF, and therefore it provides a practical way to evaluate the effective carrier lifetime after AZO sputtering.

To study the effect of AZO sputtering on effective carrier lifetime in symmetrical structures the sputtering has been performed with various pressures and substrate temperatures. The lifetime measurement results are summarized in Fig. 4 and Fig. 5 for the pressure series and in Fig. 6 and Fig. 7 for the substrate temperature series. The depositions of the pressure series were performed at room temperature. The results for all samples in pressure series (Fig. 4) show qualitatively same trend: high initial lifetime after silicon layer deposition is

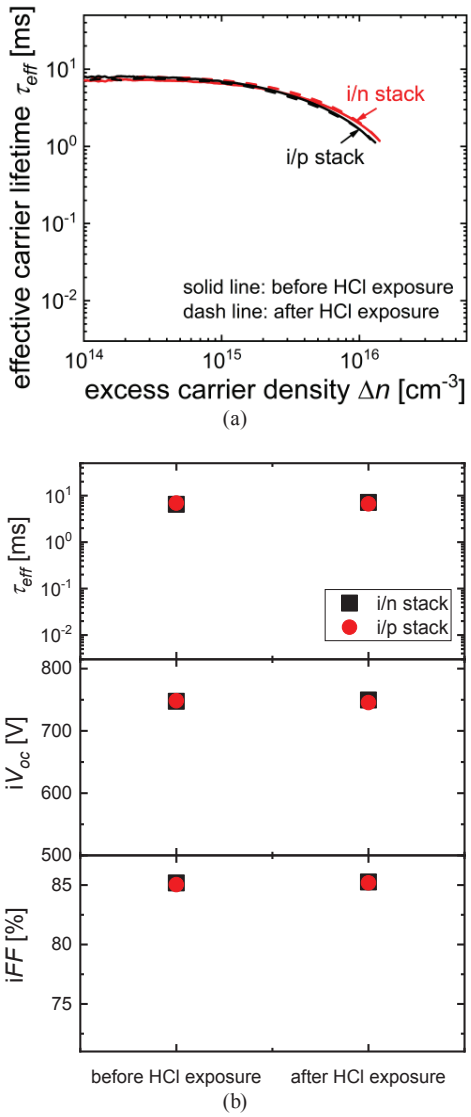

Fig. 3. Effective carrier lifetime as a function of the excess carrier density (a) and the τ_{eff}, iV_{oc}, and iFF values (b) for i/n and i/p symmetrical silicon layer stacks before and after 0.5 % HCl solution exposure

significantly reduced after AZO sputtering and mostly recovers after annealing. The samples with i/n stack show almost complete recovery after annealing and further removal of AZO slightly improves the effective carrier lifetime shown in Fig. 4 (a)-(c). However, the samples with i/p stack show incomplete

lifetime recovery after annealing in the low excess carrier density region $n < 10^{15}$ cm^{-3} which can be eliminated by AZO removal step shown in Fig. 4 (d)-(f). These results indicate that on the one hand the detrimental effect of AZO sputtering process on silicon layers can be eliminated completely by annealing, and on the other hand, the presence of AZO film reduces the effective carrier lifetime in the low excess carrier density region. This latter reduction could result from the work function mismatch between AZO and silicon layer which contributed to the reduction of field effect passivation [30]. A set of parameters τ_{eff}, iV_{oc}, and iFF evaluated out of the lifetime dependencies in Fig 4 is summarized in Fig. 5 on the sample history scale for i/n and i/p symmetrical structures. Colors and symbols in Fig. 5 represent three different pressures during AZO sputtering preformed at room temperature. The evolution of all three parameters with sample treatment steps naturally

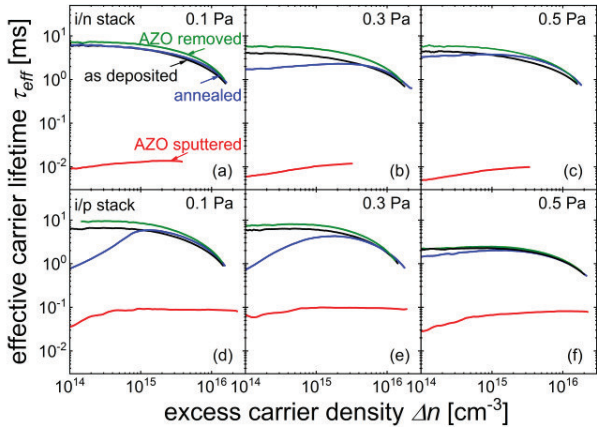

Fig. 4. Effective carrier lifetime as a function of the excess carrier density for the symmetrical stacks i/n (a)-(c) and i/p (d)-(f) with the treatment procedure: silicon layer stack deposition - AZO sputtering - annealing - AZO removal. The experiments have been performed with three different AZO sputtering pressures: 0.1, 0.3, and 0.5 Pa as noted in each graph at room temperature.

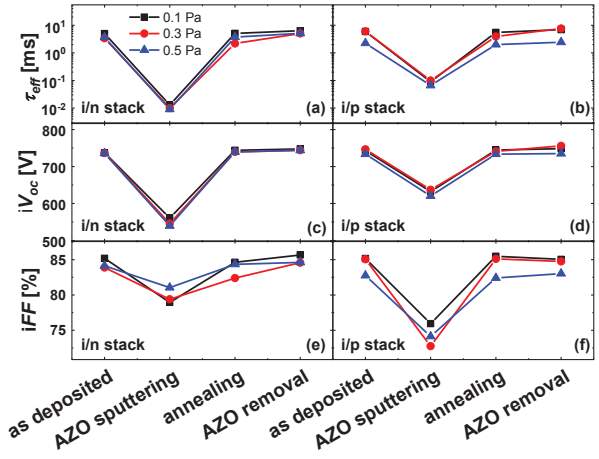

Fig. 5. The τ_{eff}, iV_{oc}, and iFF values for i/n stack (a), (c), (e) and i/p stack (b), (d), (f) at different steps of the treatment procedure: silicon layer stack deposition - AZO sputtering - annealing - AZO removal. The values are evaluated from the QSSPC data presented in the Fig. 4.

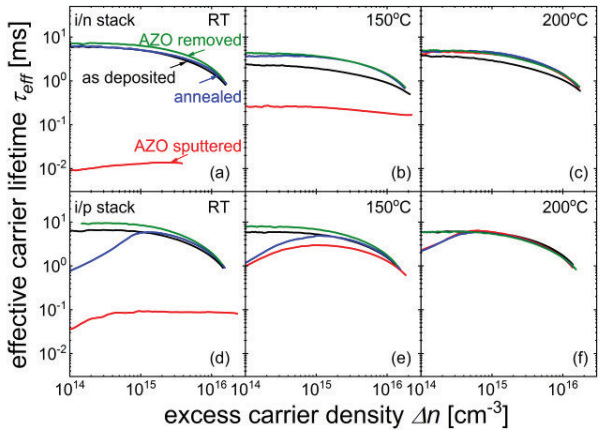

Fig. 6. Effective carrier lifetime as a function of the excess carrier density for the symmetrical stacks i/n (a)-(c) and i/p (d)-(f) with the treatment procedure: silicon layer stack deposition - AZO sputtering - annealing - AZO removal. The experiments have been performed with three different substrate temperatures: RT, 150 °C, and 200 °C as noted in each graph with pressure of 0.1 Pa.

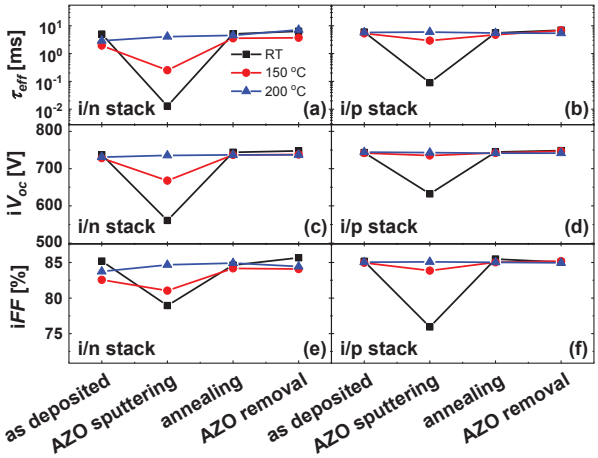

Fig. 7. The τ_{eff}, iV_{oc}, and iFF values for i/n stack (a), (c), (e) and i/p stack (b), (d), (f) at different steps of the treatment procedure: silicon layer stack deposition - AZO sputtering - annealing - AZO removal. The values are evaluated from the QSSPC data presented in the Fig. 6

follows the trend of the lifetime curves in Fig. 4 and is almost identical for all three pressures of AZO sputtering. High initial values of τ_{eff}, iV_{oc}, and iFF undergo sharp reduction after the AZO sputtering. The τ_{eff} is reduced by four orders of magnitude in i/n stack and three orders in i/p stack. The iV_{oc} qualitatively repeats the trend of τ_{eff} with stronger degradation in i/n stack. The iFF degrades stronger in i/p stack. The annealing recovers all three parameters approximately to the initial level and further AZO removal does not have any systematical impact. Note that the incomplete recovery at low carrier density in i/p stacks shown in Fig. 4 has no influence on iV_{oc} or iFF. In summary the pressure variation did not alter neither the detrimental effect of AZO sputtering on the τ_{eff}, iV_{oc}, and iFF nor the way it recovered upon annealing.

In contrast to the gas pressure, increase of substrate temperature in AZO sputtering process has an obvious influence on both i/n and i/p symmetrical samples as presented in Fig. 6 and Fig. 7. The degradation of the effective carrier

lifetime after the AZO sputtering at 150 °C is much smaller as compared to the RT process, and at 200 °C there was no degradation observed. Qualitatively the effect of the elevated substrate temperature is consistent with the fact that the degradation of the effective carrier lifetime can be eliminated by annealing. The degradation observed in the samples after AZO sputtering at RT and at 150 °C has been eliminated by post-deposition annealing. Consistently in the samples with AZO sputtered at 200 °C no influence of post-deposition annealing has been observed.

Comparing i/n and i/p stacks in Fig. 6 it can be seen that the evolutions of the lifetime curves with the treatment steps are similar for each sputtering temperature. The only exception is the case of annealing with AZO. Incomplete lifetime recovery in the i/p symmetrical stacks was observed at the low excess carrier density, similar to the results presented in Fig. 4. This bend in the lifetime curves vanished after the AZO removal in all cases and is therefore related to the presence of AZO rather than to the sputtering process.

Further evaluation of the effective carrier lifetime data of the substrate temperature series is presented in the Fig. 7 where τ_{eff}, iV_{oc}, and iFF are plotted versus the sample treatment steps. The substrate temperature during AZO sputtering has evident impact on the degradation of τ_{eff}, iV_{oc}, and iFF. The samples processed at RT show the highest degree of degradation, the samples processed at 150 °C show smaller degradation, and no effect is observed in the samples processed at 200 °C. However, the degradation discrepancies among the samples with different AZO sputtering temperatures are eliminated by the annealing. Further AZO removal does not have any noticeable effect. All dependencies converge in Fig. 7 after annealing. Therefore we consider RT AZO sputtering as a viable option for SHJ solar cell production for the cases when Ag-paste curing or other annealing step is present.

The degradation of the passivation quality after AZO sputtering process can be related to either ion bombardment damage [31] or light-induced degradation from the plasma luminescence, especially in the UV region [32]. Resolution of these two effects is in the scope of our future work. Our observations of the lifetime recovery by annealing are in line with literature reports on SHJ prepared with ITO and a-Si:H doped layers [33].

C. Effective carrier lifetime in cell structures and solar cell performance

In parallel to the experiments performed on symmetrical stacks, the effective carrier lifetime evolution has been tested in the solar cell precursor with i/n stack at the front and i/p stack at the rear. The results of QSSPC measurements on the cell precursor performed after the silicon stack deposition, after RT AZO sputtering, and after annealing are presented in Fig. 8 (a). The related values of τ_{eff}, iV_{oc}, and iFF are presented in Fig. 8 (b). Similar to the results presented in Fig. 4 the effective carrier lifetime drops severely after AZO sputtering, recovers after annealing, and shows incomplete recovery at low excess carrier density due to the i/p stack. The variations of the τ_{eff}, iV_{oc}, and iFF values presented in Fig. 8 (b) follow the trend of the lifetime variation: degrade severely after AZO sputtering and

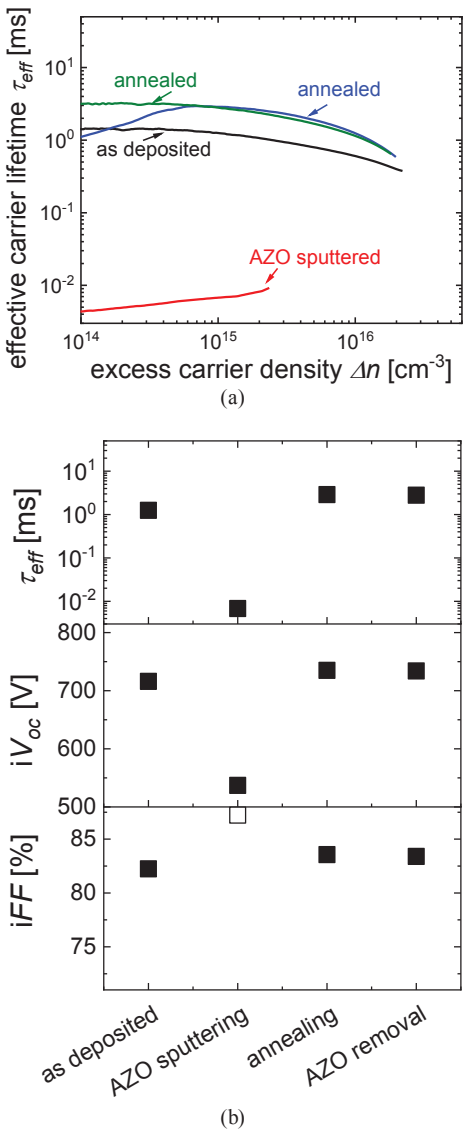

Fig. 8. Effective carrier lifetime as a function of the carrier density (a) and the τ_{eff}, iV_{oc}, and iFF values (b) for solar cell precursor with the treatment procedure: silicon layer stack deposition - AZO sputtering - annealing - AZO removal

recover after annealing. Note that unusually high value of iFF after AZO sputtering with the open symbol is an artifact of evaluation due to extremely low lifetime and therefore weak response in QSSPC measurement. Along with the data on symmetrical stacks presented in Figures 4-7 the QSSPC results of the solar cell stack show that with proper annealing, RT sputtered AZO can be applied to produce SHJ solar cells.

Finally, the 19 mm × 19 mm aperture area SHJ solar cells were fabricated with nc-Si:H<n> layer as window layer and RT sputtered AZO as TCO contacts. The cell efficiency of 21.2 % was achieved with V_{oc} = 720 mV, J_{sc}= 39.1 mA/cm^2 and FF = 75.4 %.

The V_{oc} in the cell is 15 mV below the iV_{oc} of 735 mV. The difference is attributed to the sample geometry with high ratio of perimeter to area resulting in high recombination in the perimeter region [34] and non-ideal carrier selectivity of the selective contact stacks [35], [36]. The EQE and reflection

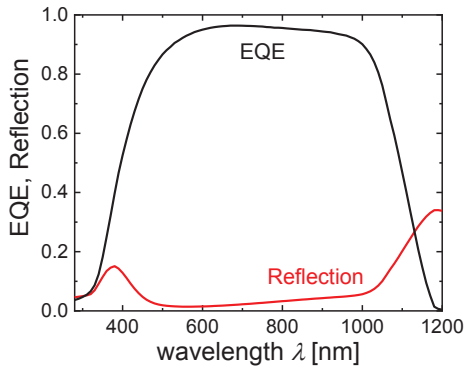

Fig. 9. External quantum efficiency (EQE) and reflection spectra of the SHJ solar cells with nc-Si:H<n> layer and RT sputtered AZO

spectra for the cell are shown in Fig. 9. The integrated J_{sc} from EQE is 38.6 mA/cm^2 which deviates from the J_{sc} of 39.1 mA/cm^2 obtained from I-V measurement by 1.3 % due to the measurement error from the different light sources and metal fractions in the illumination area. A loss of 3.2 % in *FF* from i*FF* of 83.5 % to pseudo *FF* (p*FF*) of 80.3 % obtained from J_{sc}-V_{oc} measurement is due to the recombination in selective contact stacks and the shunt resistance which contributes merely 0.1 % [37]. A loss of 4.9 % in *FF* from p*FF* to *FF* is due to the high series resistance of 1.3 Ω·cm^2 from the non-optimal screen printing.

Though the cell parameters require further optimization the achieved performance shows viability of room temperature sputtered AZO application in mass production of SHJ solar cells.

IV. Conclusion

Considering the mass production requirements, we explore the potential of implementing AZO prepared at room temperature (RT) with common magnetron sputtering technique in SHJ solar cells. We present a detailed study on the influence of the AZO sputtered at different pressures and temperatures on the effective carrier lifetime in symmetrical structures and SHJ solar cell precursors. Significant reduction of the effective carrier lifetime has been observed after the AZO sputtering at room temperature. This effect is mostly related to the sputtering process. Variation of the gas pressures during sputtering has no influence on the degree of lifetime degradation. However, the degradation of the effective carrier lifetime after the AZO sputtering is reduced for the AZO sputtered at 150 °C and eliminated for the AZO sputtered at 200 °C. The effective carrier lifetime degradation related to AZO sputtering is reduced or avoided by the in-situ annealing during sputtering process or the post-deposition annealing which is consistent with typical silver paste curing step. At last the RT sputtered AZO was applied in a rear emitter SHJ solar cell with n-type nanocrystalline silicon window layer. The cell shows an efficiency of 21.2 % with an aperture area of 19 mm × 19 mm. The most important optimization directions for the cell improvement are the reduction of V_{oc} and *FF* losses. With these results we demonstrate potential of the earth abundant and environmentally friendly AZO prepared with room temperature magnetron sputtering for industry scale SHJ solar cell production.

Acknowledgment

We would like to thank Manuel Pomaska, Karsten Bittkau, Shenghao Li, Alain Doumit, Malte Köhler, Silke Lynen, Sandra Moll, Andreas Mück, Wilfried Reetz, Hildegard Siekmann, Sven Schiffer, Andreas Schmalen, Johannes Wolff and Brigitte Zwaygardt for the technical support and Friedhelm Finger for the proof reading.

References

[1] D. Adachi, J. L. Hernandez, and K. Yamamoto, "Impact of carrier recombination on fill factor for large area heterojunction crystalline silicon solar cell with 25.1% efficiency," *Appl. Phys. Lett.,* Vol. 107, pp. 233506, 2015.

[2] M. Zeman, and D. Zhang, "Heterojunction Silicon Based Solar Cells," in Physics and Technology of Amorphous-Crystalline Heterostructure Silicon Solar Cells, W. G. J. H. M. van Sark, L. Korte, and F. Roca, Eds. Springer-Verlag, Berlin, GER, 2012, pp. 13.

[3] M. Taguchi, A. Yano, S. Tohoda, K. Matsuyama, Y. Nakamura, T. Nishiwaki, K. Fujita, and E. Maruyama, "24.7% Record Efficiency HIT Solar Cell on Thin Silicon Wafer," *IEEE J. Photovolt.,* vol. 4, no. 1, pp. 96-99, Jan. 2014.

[4] Kaneka Corporation, News Release, World's Highest Conversion Efficiency of 26.33% Achieved in a Crystalline Silicon Solar Cell –A World First in a Practical Cell Size–, JPN, Sep. 14, 2016. Available: http://www.kaneka.co.jp/en/images/topics/1473811995/1473811995_101.pdf.

[5] R. Bel Hadj Tahar, T. Ban, Y. Ohya, and Y. Takahashi, "Tin doped indium oxide thin films: Electrical properties," *J. Appl. Phys.,* vol. 83, pp. 2631-2644, 1998.

[6] V. A. Dao, H. Choi, J. Heo, H. Park, K. Yoon, Y. Lee, Y. Kim, N. Lakshminarayan, and J. Yi, "rf-Magnetron sputtered ITO thin films for improved heterojunction solar cell applications," *Current Applied Physics,* vol. 10, no. 3, pp. S506-S509, May. 2010.

[7] T. Minami, "Present status of transparent conducting oxide thin-film development forIndium-Tin-Oxide (ITO) substitutes," *Thin Solid Films,* vol. 516, no. 17, pp. 5822-5828, Jul. 2008.

[8] M. Frenzel, C. Mikolajczak, M. A. Reuter, and J. Gutzmer, "Quantifying the relative availability of high-tech by-product metals–The cases of gallium, germanium and indium," *Resources Policy,* vol. 52, pp. 327-335, Jun. 2017.

[9] V. M. Fthenakis, S. C. Morris, P. D. Moskowitz, and D. L. Morgan, "Toxicity of Cadmium Telluride, Copper Indium Diselenide, and Copper Gallium Diselenide," *Prog. Photovolt: Res. Appl.,* Vol. 7, pp. 489-497, 1999.

[10] M. A. Green, "Estimates of Te and In prices from direct mining of known ores," *Prog. Photovolt: Res. Appl.,* vol. 17, pp. 347-359, 2009.

[11] S. de Wolf, A. Descoeudres, Z. C. Holman, and C. Ballif, "High-efficiency silicon heterojunction solar cells: A review,"*Green,* vol.2, pp. 7-24, 2012.

[12] Z. A. Wang, J. B. Chu, H. B. Zhu, Z. Sun, Y. W. Chen, and S. M. Huang, "Growth of ZnO:Al films by RF sputtering at room temperature for solar cell applications," *Solid-State Electronics,* vol. 53, pp. 1149-1153, Nov. 2009.

[13] O. M. Ghahfarokhi, K. Chakanga, S. Geissendoerfer, O. Sergeev, K. von Maydell, and C. Agert, "DC-sputtered ZnO:Al as transparent conductive oxide for silicon heterojunction solar cells with μc-Si:H emitter," *Prog. Photovolt: Res. Appl.,* vol. 23, pp. 1340-1352, 2015.

[14] O. M. Ghahfarokhi, P. M. Rajanna, O. Sergeev, K. von Maydell, and C. Agert, "Effect of the Vertical Transportation Component of the TCO Layer on the Electrical Properties of

Silicon Heterojunction Solar Cells,"*IEEE J. Photovolt.,* vol. 4, no. 3, pp. 859-865, May. 2014.
[15] T. Minami, H. Nanto, and S. Takata, "Optical Properties of Aluminum Doped Zinc Oxide Thin Films Prepared by RF Magnetron Sputtering," *Jpn. J. Appl. Phys.,* vol. 24, pp. L605-L607, 1985.
[16] T. Tsuji, and M. Hirohashi, "Influence of oxygen partial pressure on transparency and conductivity of RF sputtered Al-doped ZnO thin films," *Applied Surface Science,* vol. 157, pp. 47-51, Mar. 2000.
[17] C. Agashe, O. Kluth, J. Huepkes, U. Zastrow, B. Rech, and M. Wuttig, "Efforts to improve carrier mobility in radio frequency sputtered aluminum doped zinc oxide films," *J. Appl. Phys.,* vol. 95, no. 4, pp. 1911-1917, 2004.
[18] F. Ruske, M. Roczen, K. Lee, M. Wimmer, S. Gall, J. Huepkes, D. Hrunski, and B. Rech, "Improved electrical transport in Al-doped zinc oxide by thermal treatment,"*J. Appl. Phys.,* vol. 107, pp. 013708, 2010.
[19] D. Meza, A. Cruz, A. B. Morales-Vilches, L. Korte, and B. Stannowski, "Aluminum-Doped Zinc Oxide as Front Electrode for Rear Emitter Silicon Heterojunction Solar Cells with High Efficiency," *Appl. Sci.*, vol. 9, pp. 862, 2019.
[20] A. Cruz, S. Neubert, A. B. Morales-Vilches, D. Erfurt, S. Körner, F. Ruske, B. Stannowski, B. Szyszka, and R. Schlatmann, "Optoelectronic Peformance of TCO on Silicon Heterojunction Rear-emitter Solar Cells," in 35thEUPVSEC, Brussels, Belgium, 2018.
[21] M. Huang, Z. Hameiri, A. G. Aberle, and T. Mueller, "Comparative study of amorphous indium tin oxide prepared by pulsed-DC and unbalanced RF magnetron sputtering at low power and low temperature conditions for heterojunction silicon wafer solar cell applications," *Vacuum,* vol. 119, pp. 68-76, Sep. 2015.
[22] H. Li, W. Duan, A. Lambertz, J. Hüpkes, K. Ding, F. Finger, U. Rau, and O. Astakhov, "Application of Room Temperature Sputtered Al-doped Zinc Oxide in Silicon Heterojunction Solar Cells," in WCPEC-7, Waikoloa Village, HI, USA, 2018, pp. 2151-2154.
[23] B. Y. Oh, M. C. Jeong, D. S. Kim, W. Lee, and J. M. Myoung, "Post-annealing of Al-doped ZnO films in hydrogen atmosphere," *Journal of Crystal Growth,* vol. 281, pp. 475-480, Aug. 2005.
[24] B. L. Zhu, X. Z. Zhao, F. H. Su, G. H. Li, X. G. Wu, J. Wu, and R. Wu, "Low temperature annealing effects on the structure and optical properties of ZnO films grown by pulsed laser deposition," *Vacuum,* vol. 84, pp. 1280-1286, Jun. 2010.
[25] M. Berginskia, J. Hüpkes, W. Reetz, B. Rech, and M. Wuttig, "Recent development on surface-textured ZnO:Al films preparedby sputtering for thin-film solar cell application," *Thin Solid Films,* vol. 516, no. 17, pp. 5836-5841, Jul. 2008.
[26] M. Bivour, S. Schröer, M.Hermle, S. W. Glunz, "Silicon heterojunction rear emitter solar cells: Less restrictions on the optoelectrical properties of front side TCOs,"*Solar Energy Materials & Solar Cells*, vol. 122, pp. 120-129, 2014.
[27] V. Smirnov, S. Reynolds, F. Finger, R. Carius, and C. Main, "Metastable effects in silicon thin films: Atmospheric adsorption and light-induced degradation," *Journal of Non-Crystalline Solids,* vol. 352, pp. 1075-1078, Jun. 2006.
[28] F. Finger, R. Carius, T. Dylla, S. Klein, S. Okur, and M. Guenes, "Stability of microcrystalline silicon for thin film solar cell application," *IEEE Proc.-Circuits Devices Syst.,* vol. 150, no. 4, pp. 300-308, Aug. 2003.
[29] L. H. Xiao, O. Astakhov, F. Finger, and M. Stutzmann, "Determination of the defect density in thin film amorphous and microcrystalline silicon from ESR measurements: The influence of the sample preparation procedure," *Journal of Non-Crystalline Solids,* vol. 358, no. 17, pp. 2078-2081, Sep. 2012.
[30] R. Roessler, C. Leendertz, L. Korte, N. Mingirulli, and B. Rech, "Impact of the transparent conductive oxide work function on injection-dependent a-Si:H/c-Si band bending and solar cell parameters," *J. Appl. Phys.,* vol. 113, pp. 144513, 2013.
[31] A. Illiberi, P. Kudlacek, A. H. M. Smets, M. Creatore, and M. C. M. van de Sanden, "Effect of ion bombardment on the a-Si:H based surface passivation of c-Si surfaces," *Appl. Phys. Lett.,* vol. 98, pp. 242115, 2011.
[32] F. Lebreton, S. N. Abolmasov, F. Silva, and P. R. i Cabarrocas, "In situ photoluminescence study of plasma-induced damage at the a-Si:H/c-Si interface,"*Appl. Phys. Lett.,* vol. 108, pp. 051603, 2016.
[33] A. Morales-Vilches, C. Voz, M. Colina, G. López, I. Martín, P. Ortega, A. Orpella, and R. Alcubilla, "Recovery of indium-tin-oxide/silicon heterojunction solar cells by thermal annealing,"*Energy Procedia,* vol. 44, pp. 3-9, 2014.
[34] F. Haase, S. Schaefer, C. Klamt, F. Kiefer, J. Kruegener, R. Brendel, and R. Peibst, "Perimeter Recombination in 25%-Efficient IBC Solar Cells With Passivating POLO Contacts for Both Polarities," *IEEE J. Photovolt.,* vol. 8, no. 1, pp. 23-29, Jan. 2018.
[35] M. Bivour, M. Reusch, F. Feldmann, M. Hermle, and S. Glunz, "Requirements for Carrier Selective Silicon Heterojunctions," in 24th Workshop on Crystalline Silicon Solar Cells & Modules: Materials and Processes, Colorado, USA, 2014
[36] P. Koswatta, M. Boccard, and Z. Holman, "Carrier-Selective Contacts in Silicon Solar Cells,", in 2015 IEEE 42nd Photovoltaic Specialist Conference (PVSC), New Orleans, LA, USA, 2015.
[37] A. Khanna, T. Mueller, R. A. Stangl, B. Hoex, P. K. Basu, and A. G. Aberle, "A Fill Factor Loss Analysis Method for Silicon Wafer Solar Cells," *IEEE J. Photovolt.,* vol. 3, no. 4, pp. 1170-1177, Oct. 2013.